SURFACE FEMTOCHEMISTRY: WHAT IS THE ROLE OF SUBSTRATE ELECTRONS?

R.J. FINLAY, T.-H. HER, S. DELIWALA, W.D. MIEHER, C. WU, AND E. MAZUR
Gordon McKay Laboratory, Harvard University, Cambridge, MA 02138, USA

ABSTRACT

The desorption of O_2 from O_2/Pt(111) and the formation of CO_2 from CO/O_2/Pt(111) are measured following excitation at various laser wavelengths with pulse durations from 80-fs to 3.6-ps. The trends in the reaction yield reflect a reaction mechanism in which substrate electrons out of thermal equilibrium interact with the adsorbates. We also demonstrate a rudimentary control of branching ratio using subpicosecond ultraviolet laser pulses.

1. Introduction

We studied the desorption of O_2 and formation of CO_2 initiated with subpicosecond laser pulse excitation of O_2/Pt(111) and coadsorbed CO/O_2/Pt(111) surfaces at 90 K in ultrahigh vacuum. O_2 desorption and laser-induced CO_2 formation (followed by desorption) are detected with a mass spectrometer. The surface chemistry of the O_2/Pt(111) and CO/O_2/Pt(111) systems has been well characterized.[1-3] The photochemistry of these systems has been studied with arc lamp irradiation,[4, 5] and with nanosecond[6, 7] and subpicosecond[6, 8] laser pulses. We report the fluence dependence of the desorption yield of O_2 and CO_2 at 267, 400, and 800 nm over a range of pulsewidths from 100 fs to 3.6 ps. We also present two-pulse correlation data obtained with 80-fs pulses at 800 nm using delays up to 75 ps. The experiments reported in this paper extend the range of excitation conditions used in previously published studies. The results provide convincing evidence that nonthermalized highly-excited electrons play a significant role in the desorption and surface reaction processes. In addition we show rudimentary control of the branching ratio between desorption of O_2 and formation of CO_2.

Previous experiments[6, 8-11] established that desorption from metal surfaces induced by subpicosecond laser pulses has a highly nonlinear dependence on the laser fluence. Although the lifetime of the excited electrons in the metal substrate is on the order of a picosecond,[12, 13] it has been reported that the desorption process occurs in less than 325 fs.[14] Both the nonlinear fluence dependence and the short time scale of the desorption have been attributed to hot electrons in the metal.[6, 8-11, 13-15]

2. Experiment

A Pt(111) surface is cleaned and prepared in ultrahigh vacuum using established methods.[4] The clean Pt surface is dosed to saturation (0.44 monolayers[16]) with $^{18}O_2$ utilizing a capillary array to minimize the O_2 background pressure during the

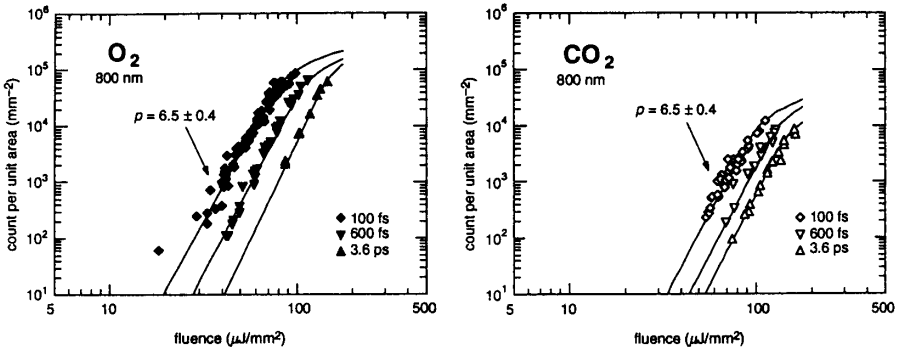

Fig. 1. Pulsewidth dependence of the laser induced desorption from O_2/Pt(111) and CO_2 formation from CO/O_2/Pt(111) for 800-nm pulses of 100-fs (◆◇), 0.6-ps (▼▽), and 3.6-ps (▲△) duration. The power-law exponent is 6.5 ± 0.4, independent of pulsewidth. The exponent is the same for O_2 desorption as for CO_2 formation.

experiment. For the mixed layer CO/O_2/Pt(111), a 3 × 10^{-6} Torr-s background exposure of $^{12}C^{18}O$ follows the $^{18}O_2$ dose. Below 100 K, O_2 chemisorbs molecularly on Pt(111) in atop and bridge sites with the O–O bond axis parallel to the surface and bond orders of about 1.[16] In the presence of preadsorbed O_2, CO has been observed in the atop sites.[4]

The experiments employ a regeneratively amplified Ti:sapphire laser system designed in our laboratory. The system employs chirped-pulse amplification and all-reflective optics to produce 0.5-mJ, 800-nm pulses of 80-fs duration at a 1-kHz repetition rate. Chirped pulses of longer duration can be obtained by adjusting the pulse compressor. Frequency-doubling the 800-nm pulses in a 1-mm long LBO crystal yields 0.1-mJ, 400-nm pulses of 0.2-ps duration and sum-frequency mixing of the 800 and 400-nm pulses in a 0.3-mm long BBO crystal yields 17-μJ pulses at 267 nm. We estimate a pulsewidth of 0.35 ps for the 267-nm pulses based on the group velocities of the 400 and 800-nm pulses in BBO.

The fluence is calibrated for each data run by measuring the energy and spatial profile of the laser pulses. The energy is measured with a photodiode referenced to a calibrated pyroelectric detector. Typical shot-to-shot energy fluctuations are 2% at 800 nm, 5% at 400 nm, and 10% at 267 nm. A CCD camera measures the profile of the 800 and 400-nm pulses. The profile of the 267-nm pulses is measured by scanning a 25-μm pinhole through the beam. The measured spatial profile is numerically fit to an elliptical Gaussian function to obtain absorbed fluence at the center of the laser spot. For all wavelengths the absorbed fluence (*i.e.*, the incident fluence times the absorption of platinum[17]) is in the range 10-200 $\mu J/mm^2$. For 400 and 800-nm pulses, the fluence is varied by changing the total incident energy with a half-wave plate and a polarizer. At 267 nm, the incident energy is held constant and a lens is displaced to change the spot size on the sample. Each time the lens is moved, the spatial profile of the beam is measured.

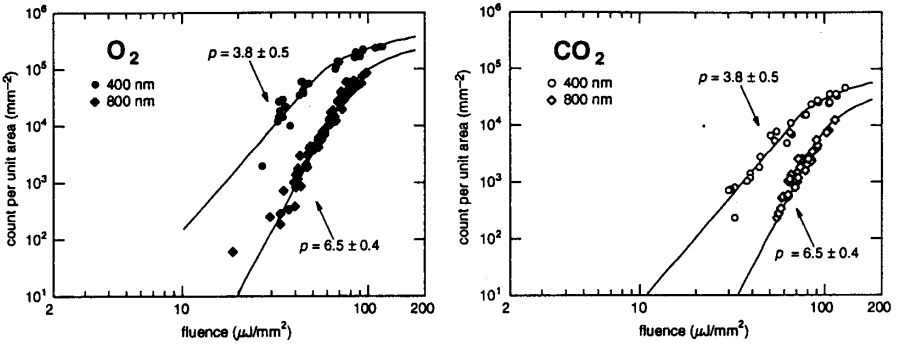

Fig. 2. Wavelength dependence of the laser-induced O_2 and CO_2 yields. Yields from 400-nm (●○) 0.2-ps, and 800-nm (◆◇) 100-fs pulses have different power law exponents. The curves are obtained from a power law which accounts for saturation of the yield due to the finite number of molecules within the laser spot.

We measure the time-integrated mass spectrometer signal as a function of laser fluence, wavelength, pulse duration, and pulse sequence. Between laser shots the sample is translated by twice the FWHM of the irradiated area so that each data point is from a fresh spot on the sample. When the entire sample has been used, the sample is cleaned and redosed. A negatively biased grid in front of the mass spectrometer shields the sample from stray electrons from the ionizer. A mechanical shutter is used to increase the time interval between successive laser shots to 0.4 s to allow the mass spectrometer signal to return to the background level.

The experimental results are shown in Figs. 1 through 4. In Figs. 1 through 3, each data point represents the yield per unit area obtained from the first laser shot taken at a fresh spot on the Pt sample. Figure 1 shows the O_2 desorption and CO_2 reaction yields from 800-nm pulses of 100-fs, 0.6-ps, and 3.6-ps durations. The steep slope of the data, 6.5 ± 0.4 for both O_2 and CO_2, is unchanged with pulsewidth. Figure 2 compares the desorption and reaction yields induced with 100-fs, 800-nm and 0.2-ps, 400-nm pulses. The slope of the data at 400 nm is 3.8 ± 0.5 for both O_2 and CO_2. The nearly identical fluence dependence of the O_2 and CO_2 data provides strong evidence for a common excitation mechanism for desorption of O_2 and formation of CO_2. The ratio in desorption yield of O_2 to CO_2 is about 10, in sharp contrast with the ratio of 0.5 found with nanosecond irradiation.[3] The curves through the data are power laws relating yield to fluence, with the yield limited by the number of molecules on the surface. At low fluences, $Y \propto F^p$ but at higher fluences the curves flatten out to reflect the saturation of the yield.[18]

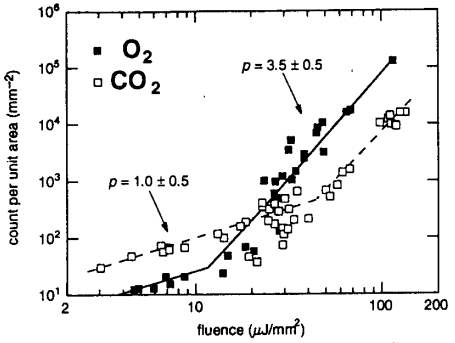

Fig. 3. Laser-induced desorption of O_2 (■) and formation of CO_2 (□) with 0.35-ps 267-nm laser pulses. Lines through the data indicate the onset of the nonlinear reaction mechanism and a corresponding change in the O_2:CO_2 branching ratio.

Figure 3 shows the desorption and reaction yields induced by the 267-nm pulses. At high fluence there is a nonlinear relationship between the yield and fluence: the lines through the high fluence data have slopes of 3.5. In this fluence regime, the ratio of O_2 to CO_2 yield is close to 10. At low fluence, near 25 $\mu J/mm^2$, there is a crossover in the O_2 to CO_2 yields and the ratio of the yields changes to 0.2. This is the first time that subpicosecond laser pulses have been used to promote reaction more efficiently than desorption.

Figure 4 shows the total desorption yield for two 80-fs, 800-nm pulses as a function of the delay t_1–t_2 between them. With equal absorbed fluence in the two pulses the correlation is symmetric; with unequal fluences an asymmetry appears in the wings as previously reported. The central peak has a full-width at half-maximum of 1.8 ps and is attributed to the cooling of hot substrate electrons by diffusion and coupling to the lattice.[8, 10, 11] The dashed line shows the total yield when the two pulses act independently, *i.e.*, when t_1–$t_2 \rightarrow \infty$. The observed 0.1-ns decay time of the wings shows that the excitation lasts longer than the electron-adsorbate,[13, 19] electron-lattice,[11-14] and lattice-adsorbate[20] relaxation times. This long decay can only be attributed to the cooling of the surface to the bulk, which occurs roughly on a 0.1-ns time-scale.

3. Discussion

The wavelength- and time-dependence of the data shown in Figs. 1-4 allow us to determine at what stage in the relaxation of the substrate excitation the surface chemistry occurs. The response of the metal substrate to an ultrashort laser pulse is sketched in Fig. 5 with a series of graphs showing the evolution of the electron distribution. Before the excitation the lattice and electrons are in equilibrium with each other at 90 K (*a*). The laser pulse excites electrons to a range of states above the Fermi level (*b*). The nonequilibrium electron distribution shown is for illustrative purposes only; the actual distribution is determined by the Pt band

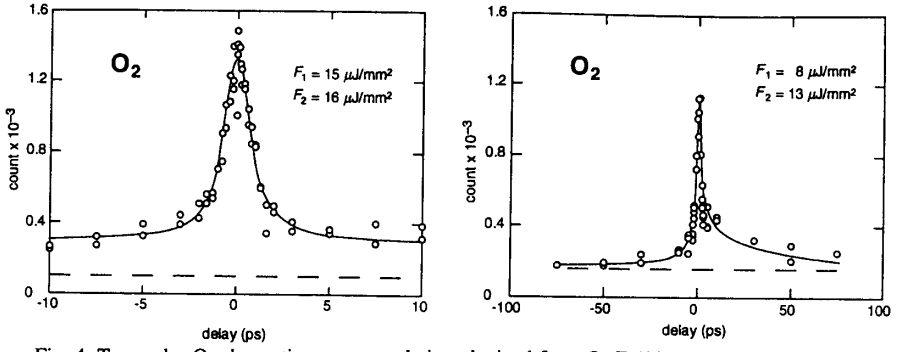

Fig. 4. Two-pulse O_2 desorption crosscorrelation obtained from O_2/Pt(111) with 80-fs, 800-nm pulses. With unequal absorbed fluences (right), the cross-correlation is asymmetric. The dashed lines indicate the total measured yield for two pulses separated by infinite delay.

structure, and the laser wavelength and pulse duration. Rapid thermalization causes electrons and holes to converge towards the Fermi level (*c*); for typical laser pulse energies the resulting hot electron distribution reaches 2000 K. In the following few picoseconds, the electrons cool as they equilibrate with the surface lattice; this heats the lattice and cools the electrons to a common temperature near 200 K (*d*). Over the following tens of picoseconds, the hot lattice at the surface returns to the bulk Pt temperature of 90 K (*e*).

The nonlinear desorption induced by ultrashort pulses has been attributed to a coupling between adsorbate vibrational modes and the thermalized hot electrons in stage *c*.[9, 11, 13, 14, 19, 21] Though this neglects the nonequilibrium electron distribution produced by the laser excitation, models based upon thermalized electrons successfully account for the nonlinear dependence of yield on fluence and the short timescale observed in the crosscorrelation.[10, 19, 21]

These models, however, are inconsistent with the observed wavelength dependence in Figs. 2 and 3. Since the absorption depth in Pt is nearly constant over the range 267 to 800 nm, the peak electron temperature of the thermalized electron distribution depends only on absorbed energy and not on photon energy. At fixed absorbed fluence, laser pulses at any wavelength between 267 and 800 nm create nearly identical thermalized electron distributions which would lead to wavelength-independent surface chemistry. The slightly different pulsewidths used at the three excitation wavelengths in this experiment (from 70 fs at 800 nm to 0.35 ps at 267 nm) cannot account for the observed dependence of the power law exponent on wavelength, because as Fig. 1 demonstrates the power law exponent is independent of pulsewidth.

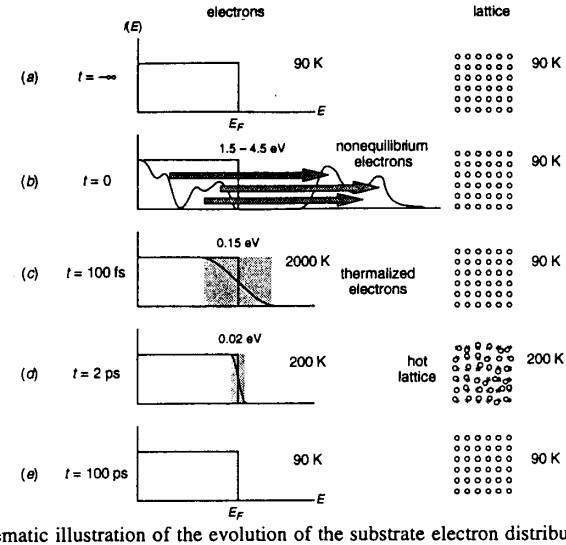

Fig. 5. A schematic illustration of the evolution of the substrate electron distribution and lattice excitation. *a* Initially the electrons and lattice are in equilibrium at 90 K. *b* The light creates a nonequilibrium electron distribution which *c* becomes a distribution of thermalized electrons. *d* The electrons cool to produce a hot lattice at the substrate surface. *e* The surface cools to the bulk temperature in about 0.1 ns.

This leads us to conclude that one cannot ignore the nonequilibrium electron distribution produced by the laser excitation. In contrast to the thermalized distribution, the nonequilibrium distribution is sensitive to photon energy, see Fig. 5*b*. The observed wavelength dependence could therefore arise from nonequilibrium electrons. Theoretical models of the chemistry must account for the wavelength dependence of the nonequilibrium electron distribution by incorporating the Pt band structure and relaxation of the nonequilibrium electron distribution towards a Fermi distribution.

The cross-correlation data in Fig. 4 show two correlation timescales that are substantially longer than the lifetime of the nonequilibrium electrons. The short correlation timescale (< 2 ps) is similar to the period over which the electrons cool to the surface lattice temperature; the long correlation timescale (0.1 ns) is comparable to the time required for the surface to cool to the bulk.

Previous work with continuous illumination in the ultraviolet using an arc lamp source,[4, 5] and nanosecond laser illumination[6] reported CO_2 to O_2 yields in the ratio 0.5. In Fig. 2, a similar branching ratio is obtained using 0.35-ps, 267-nm laser pulses of low fluence. The change in the branching ratio from the high-fluence value of 10 and the decrease in nonlinearity of the yield reflect a change in the reaction mechanism.

4. Conclusion

Comparison of data obtained at different wavelengths shows a clear dependence of desorption yield on wavelength. This behavior cannot be adequately described by current theoretical models, which predict a dependence on absorbed fluence but not on wavelength. The observed wavelength dependence therefore calls for models that incorporate a nonthermal electron distribution.

In addition to the 1.8-ps central peak, the two-pulse experiments show a 0.1-ns decay time exceeding all relaxation times except the cooling of the surface to the bulk temperature. The observation of a two-pulse correlation signal on such a long time scale implies that the temperature of the surface plays a role in the femtosecond-laser-induced desorption process.

Ultrashort UV laser pulses (267 nm) can be used to access two reaction regimes. At high fluence, a nonlinear dependence of yield on fluence is observed in which the O_2 product exceeds the CO_2 product by a factor of $\approx$10. At less than 25 $\mu J/mm^2$ of UV fluence, CO_2 production exceeds O_2 desorption. This rudimentary control of branching ratio has practical importance in the study of time-resolved surface reaction dynamics, where conditions under which an ultrashort laser pulse can preferentially induce a surface reaction over desorption are desirable.

5. Acknowledgments

This research is supported by the Army Research Office under Contract DAAH04-95-0615 and the Joint Services Electronics Program under Contract N00014-89-J-1023. R.J.F. is supported by the Natural Science and Engineering Research Council of Canada. Generous support from Perkin-Elmer Physical Electronics, and ConOptics Inc. is gratefully acknowledged.

6. References

1. T. Matsushima, *Surf. Sci.* **127** (1983) 403.
2. T. Matsushima, *Surf. Sci.* **123** (1982) L663.
3. K.-H. Allers, H. Pfnür, P. Feulner, and D. Menzel, *J. Chem. Phys.* **100** (1994) 3985.
4. W. D. Mieher, and W. Ho, *J. Chem. Phys.* **99** (1993) 9279.
5. W. D. Mieher, and W. Ho, *J. Chem. Phys.* **91** (1989) 2755.
6. F.-J. Kao, D. G. Busch, D. Gomes da Costa, and W. Ho, *Phys. Rev. Lett.* **70** (1993) 4098.
7. V. A. Ukraintsev, and I. Harrison, *J. Chem. Phys.* **96** (1992) 6307.
8. F.-J. Kao, D. G. Busch, D. Cohen, D. Gomes da Costa, and W. Ho, *Phys. Rev. Lett.* **71** (1993) 2094.
9. J. A. Prybyla, T. F. Heinz, J. A. Misewich, M. M. T. Loy, and J. H. Glownia, *Phys. Rev. Lett.* **64** (1990) 1537.

10. F. Budde, T. F. Heinz, M. M. T. Loy, J. A. Misewich, F. de Rougemont, and H. Zacharias, *Phys. Rev. Lett.* **66** (1991) 3024.
11. J. A. Misewich, A. Kalamarides, T. F. Heinz, U. Höfer, and M. M. T. Loy, *J. Chem. Phys.* **100** (1994) 736.
12. S. I. Anisimov, B. L. Kapeliovich, and T. L. Perel'man, *Sov. Phys. JETP* **39** (1974) 375.
13. F. Budde, T. F. Heinz, A. Kalamarides, M. M. T. Loy, and J. A. Misewich, *Surf. Sci.* **283** (1993) 143.
14. J. A. Prybyla, H. W. K. Tom, and G. D. Aumiller, *Phys. Rev. Lett.* **68** (1992) 503.
15. R. R. Cavanagh, D. S. King, J. C. Stephenson, and T. F. Heinz, *J. Phys. Chem.* **97** (1993) 786.
16. H. Steininger, S. Lehwald, and H. Ibach, *Surf. Sci.* **123** (1982) 1.
17. J. H. Weaver, C. Krafka, D. W. Lynch, and E. E. Koch, *Optical Constants of Materials, Part 1, Physics Data* (1981).
18. S. Deliwala, R. J. Finlay, J. R. Goldman, T. H. Her, W. D. Mieher, and E. Mazur, *Chem. Phys. Lett.* **242** (1995) 617.
19. J. A. Misewich, T. F. Heinz, and D. M. Newns, *Phys. Rev. Lett.* **68** (1992) 3737.
20. T. A. Germer, J. C. Stephenson, E. J. Heilweil, and R. R. Cavanagh, *Phys. Rev. Lett.* **71** (1993) 3327.
21. D. G. Busch, S. Gao, R. A. Pelak, M. F. Booth, and W. Ho, *Phys. Rev. Lett.* **75** (1995) 673.